

Latent symmetry in a minimal non-Hermitian trimer

PAULO A. BRANDÃO¹

¹Instituto de Física, Universidade Federal de Alagoas, Av. Lourival Melo Mota, S/N, 57072-970, Tabuleiro do Martins, Maceió, Alagoas, Brasil.
*paulo.brandao@fis.ufal.br

Compiled March 18, 2026

We study a minimal non-Hermitian trimer with latent symmetry formed by a cospectral pair of sites embedded in a three-site network with nonreciprocal couplings. We show that the model admits an exact decomposition into dark and bright sectors: the dark mode is spectrally isolated and retains a complex eigenvalue, while the bright sector reduces to an effective non-Hermitian dimer. For a suitable choice of parameters, this reduced subsystem becomes \mathcal{PT} -symmetric and exhibits partial spectral reality, with two real eigenvalues coexisting with the complex dark eigenvalue. At the critical point, the bright sector hosts an embedded second-order exceptional point, which renders the full trimer defective and gives rise to the characteristic Jordan-block dynamics. These results establish the non-Hermitian trimer as a minimal analytically solvable setting in which latent symmetry, sector-resolved \mathcal{PT} symmetry, and exceptional-point physics naturally coexist.

<http://dx.doi.org/10.1364/ao.XX.XXXXXX>

1. INTRODUCTION

Non-Hermitian Hamiltonians have become a central tool for describing effective dynamics in open and wave-based systems with gain, loss, and asymmetric mode conversion. In particular, parity-time (\mathcal{PT}) symmetry showed that non-Hermitian operators may still display entirely real spectra within a finite parameter window, followed by a symmetry-breaking transition in which eigenvalues become complex [1, 2]. Optical settings have played a decisive role in this development because coupled waveguides, resonators, and synthetic lattices provide a flexible platform in which gain, loss, and nonreciprocal couplings can be engineered and probed directly [2–6]. A hallmark of such systems is the presence of exceptional points (EPs), non-Hermitian degeneracies at which both eigenvalues and eigenvectors coalesce, leading to defective Hamiltonians and anomalous dynamical responses [5–7].

In parallel, recent work has shown that spectral graph concepts such as cospectrality can generate a more hidden form of order in networks. Two sites are cospectral when the corresponding vertex-deleted subgraphs have the same characteristic polynomial [8, 9]. This notion underlies latent symmetry, a generalized symmetry that is not necessarily visible in the full graph but emerges after suitable spectral reduction [10]. In photonic

lattices, latent symmetry was recently shown to constrain eigenmodes and transport in a robust and experimentally accessible way, opening a new route to mode engineering beyond conventional geometric symmetries [11, 12].

These two directions suggest a natural question: how does latent symmetry manifest itself in a genuinely non-Hermitian setting? More specifically, can a minimal non-Hermitian network combine cospectrality, dark-state formation, and \mathcal{PT} -type spectral transitions in a single analytically tractable model? Addressing this question is appealing both conceptually and practically. Conceptually, latent symmetry is formulated through spectral constraints, whereas non-Hermitian physics is governed by complex spectra, defective eigenspaces, and sector-dependent stability. Practically, minimal non-Hermitian trimers already serve as canonical models for coupled photonic structures and provide the simplest setting in which one may embed a nontrivial spectator mode alongside a reduced dimer dynamics.

Nonreciprocal couplings of the kind considered here are no longer purely theoretical. In chiral quantum optics, spin-momentum locking in guided modes gives rise to propagation-direction-dependent emission, scattering, and absorption, thereby providing a natural route to effective nonreciprocal interactions in reduced models [13]. Experimentally, such chiral interfaces have been demonstrated with cold atoms coupled to optical nanofibres, where spontaneous emission into the two counter-propagating guided modes can be tuned from symmetric to strongly asymmetric [14], with semiconductor quantum dots embedded in nanophotonic waveguides, where near-unity directionality and deterministic chiral photon-emitter coupling have been achieved [15, 16], and with superconducting circuits, where on-demand directional microwave photon emission and strong unidirectional coupling have recently been reported [17, 18]. Related cascaded radiative dynamics have also been observed in waveguide-coupled atomic platforms [19]. In this sense, the asymmetric couplings employed in our minimal trimer may be viewed as an effective reduced description of experimentally accessible chiral and cascaded photonic architectures.

Several non-Hermitian trimers have been investigated in the context of \mathcal{PT} symmetry and related spectral transitions. Early work on \mathcal{PT} -symmetric oligomers established the trimer as one of the minimal few-site platforms displaying non-Hermitian phase transitions, nonlinear stationary states, and nontrivial stability properties [20]. This picture was later refined in a systematic study of the \mathcal{PT} -symmetric trimer, where bifurcations, ghost states, and the associated unstable dynamics were analyzed in detail [21]. Beyond globally \mathcal{PT} -symmetric gain-neutral-loss

arrangements, it was subsequently shown that non-Hermitian trimers may also exhibit entirely real spectra in the absence of explicit spatial \mathcal{PT} symmetry, highlighting the broader role of pseudo-Hermitian structures in few-mode systems [22]. In a different direction, trimers have also been used as parent platforms for the emergence of effective non-Hermitian dimers, for instance through adiabatic elimination in coupled waveguides [23]. More recently, triangular bosonic trimers with complex couplings have revealed the interplay between \mathcal{PT} symmetry and chiral current circulation, further emphasizing the richness of three-site non-Hermitian geometries [24]. In this context, the present work identifies a distinct minimal mechanism: rather than imposing a global \mathcal{PT} symmetry on the full trimer, we exploit latent symmetry to generate an exact dark–bright decomposition, in which the bright invariant sector reduces to an effective \mathcal{PT} -symmetric dimer while the dark mode remains spectrally isolated.

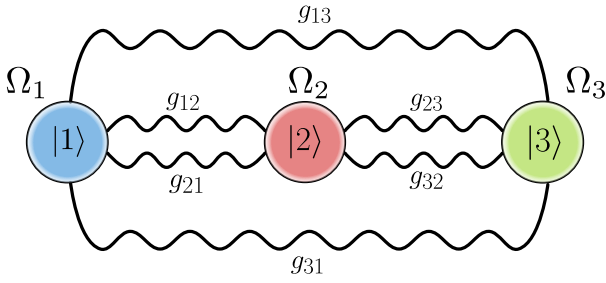


Fig. 1. Minimal non-Hermitian trimer formed by three coupled sites, $|1\rangle$, $|2\rangle$, and $|3\rangle$, with complex onsite energies $\Omega_j = \omega_j + i\gamma_j$. The pair $(|1\rangle, |2\rangle)$ becomes cospectral when $\Omega_1 = \Omega_2$ and $g_{13}g_{31} = g_{23}g_{32}$, giving rise to a latent symmetry, while site $|3\rangle$ plays the role of a singlet site.

2. TRIMER MODEL AND COSPECTRALITY

Consider a physical configuration of three connected sites $|1\rangle$, $|2\rangle$ and $|3\rangle$ having complex energies $\Omega_j = \omega_j + i\gamma_j$ ($j = 1, 2, 3$) with $\omega_j, \gamma_j \in \mathbb{R}$, as displayed in Fig. 1. The effective non-Hermitian Hamiltonian describing this configuration can be written in a tight-binding form as

$$H = \sum_{j=1}^3 \Omega_j |j\rangle \langle j| + \sum_{i=1}^3 \sum_{j \neq i}^3 g_{ij} |i\rangle \langle j|, \quad (1)$$

where g_{ij} are the real-valued coupling constants. In the basis $\{|1\rangle, |2\rangle, |3\rangle\}$, the Hamiltonian can be represented by the complex matrix

$$H = \begin{pmatrix} \omega_1 + i\gamma_1 & g_{12} & g_{13} \\ g_{21} & \omega_2 + i\gamma_2 & g_{23} \\ g_{31} & g_{32} & \omega_3 + i\gamma_3 \end{pmatrix}. \quad (2)$$

The latent symmetry of a network is constructed in terms of its cospectrality. Two sites $|i\rangle$ and $|j\rangle$ are said to be *cospectral* if the vertex-deleted subgraphs, $H \setminus |i\rangle$ and $H \setminus |j\rangle$, have the same characteristic polynomial [8–10]. Let us use this concept to develop a set of conditions such that sites $|1\rangle$ and $|2\rangle$ become cospectral. The subgraphs $H \setminus |1\rangle$ and $H \setminus |2\rangle$ obtained by removing sites $|1\rangle$ and $|2\rangle$, respectively, are represented by the

matrices

$$H \setminus |1\rangle = \begin{pmatrix} \omega_2 + i\gamma_2 & g_{23} \\ g_{32} & \omega_3 + i\gamma_3 \end{pmatrix}, \quad (3)$$

$$H \setminus |2\rangle = \begin{pmatrix} \omega_1 + i\gamma_1 & g_{13} \\ g_{31} & \omega_3 + i\gamma_3 \end{pmatrix}. \quad (4)$$

It is a simple exercise to demonstrate that the eigenvalues of the above matrices are equal if and only if

$$\omega_1 = \omega_2 = \omega, \quad \gamma_1 = \gamma_2 = \gamma \quad \text{and} \quad g_{13}g_{31} = g_{23}g_{32}. \quad (5)$$

The above conditions on the cospectrality between $|1\rangle$ and $|2\rangle$ imply that latent symmetry does not require gain-loss balance between sites 1 and 2. It only requires equal complex onsite potentials and a product constraint on the couplings. Thus, one has additional freedom regarding the coupling constants, since the last condition on Eq. (5) does not imply that the couplings g_{ij} need to be symmetric, in the sense that $g_{ij} = g_{ji}$.

Suppose that conditions given by Eq. (5) are satisfied for some particular set of parameters and that the three eigenvalues of H are nondegenerate. Then, the sites $|1\rangle$ and $|2\rangle$ exhibit a latent symmetry and the trimer is said to be latent symmetric. It is possible for a latent symmetric structure to feature singlet sites. They are defined as the set of sites whose distances (in the sense of a graph metric) to a pair of sites exhibiting a latent symmetry are equal. In our trimer model, since there is only one extra site, $|3\rangle$, it is a singlet site since it has the same distance to $|1\rangle$ and $|2\rangle$. What is interesting about singlet sites is that depending on the initial excitation on the pair $(|1\rangle, |2\rangle)$, the dynamics of $|3\rangle$ is trivial [11].

To account for the conditions given by Eq. (5), we parametrize the Hamiltonian by introducing a single deformation parameter χ and write

$$H(\chi) = \begin{pmatrix} \Omega & \mu e^{2\chi} & \kappa e^\chi \\ \mu e^{-2\chi} & \Omega & \kappa e^{-\chi} \\ \kappa e^{-\chi} & \kappa e^\chi & \Omega_3 \end{pmatrix}, \quad (6)$$

where $\Omega = \omega + i\gamma$, $\mu > 0$, $\kappa > 0$. This form is more convenient and we can study the entire dynamics in terms of Ω , μ , κ and χ . Notice that Eq. (6) is related to Eq. (2) (with the conditions discussed above) by the similarity transformation $H(\chi) \rightarrow DHD^{-1}$, where $D = \text{diag}(e^\chi, e^{-\chi}, 1)$, and so χ cannot change the eigenvalue structure of Eq. (2).

3. RESULTS AND DISCUSSION

We now demonstrate that latent symmetry divides the network into dark and bright sectors. The bright sector can exhibit a \mathcal{PT} -symmetric phase transition with real eigenvalues while the dark sector remains in the “broken” phase with a single complex eigenvalue. The easiest way to see this is by noting that $|D\rangle = e^\chi |1\rangle - e^{-\chi} |2\rangle$ is an eigenvector of $H(\chi)$ with eigenvalue $\lambda_0 = \Omega - \mu = \omega - \mu + i\gamma$. This implies that site $|3\rangle$ is invisible to the dynamics generated by the invariant subspace $\text{span}\{|D\rangle\}$, which is the dark sector of the trimer. If the initial state is given by $|\psi(0)\rangle = |D\rangle$, then $|\psi(t)\rangle = e^{-iHt} |\psi(0)\rangle = e^{-i(\omega-\mu)t} e^{\gamma t} (e^\chi |1\rangle - e^{-\chi} |2\rangle)$. Thus, the local occupations $P_j = |\langle j|\psi(t)\rangle|^2$ of sites $j = 1, 2, 3$ are given by $P_1 = e^{2\gamma t} e^{2\chi}$, $P_2 = e^{2\gamma t} e^{-2\chi}$ and $P_3 = 0$. Cospectrality

between $|1\rangle$ and $|2\rangle$ thus guarantees that if the initial excitation is antisymmetric in the latent sites $|1\rangle$ and $|2\rangle$, the amplitude P_3 always vanishes.

On the other hand, for the state $|B\rangle = (e^\chi |1\rangle + e^{-\chi} |2\rangle)/\sqrt{2}$ one has $H(\chi)|B\rangle = (\Omega + \mu)|B\rangle + \sqrt{2}\kappa|3\rangle$ and $H(\chi)|3\rangle = \sqrt{2}\kappa|B\rangle + \Omega_3|3\rangle$. Therefore, the set $\text{span}\{|B\rangle, |3\rangle\}$ generates another invariant subspace which is the bright sector. In this basis, the dynamics is described by the 2×2 matrix

$$H(\chi)_B = \begin{pmatrix} \Omega + \mu & \sqrt{2}\kappa \\ \sqrt{2}\kappa & \Omega_3 \end{pmatrix}, \quad (7)$$

which has eigenvalues

$$\lambda_{\pm} = \frac{\Omega + \Omega_3 + \mu \pm \Delta}{2}, \quad (8)$$

where $\Delta = [(\Omega + \mu - \Omega_3)^2 + 8\kappa^2]^{1/2}$. Can this bright sector generate stable evolution in the sense of having nondivergent behavior for P_j ? Since $\Omega = \omega + i\gamma$ and $\Omega_3 = \omega_3 + i\gamma_3$, we see from Eq. (8) that in order to have $\lambda_{\pm} \in \mathbb{R}$ it is necessary that

$$\gamma_3 = -\gamma \quad \text{and} \quad \omega_3 = \omega + \mu. \quad (9)$$

This condition imposes that dissipation present in mode $|3\rangle$ must be of opposite sign compared to that in modes $|1(2)\rangle$ and also that there must be a frequency mismatch between $|3\rangle$ and $|1(2)\rangle$. We assume this to be the case in what follows. The matrix given by Eq. (7) can now be written as

$$H(\chi)_B = \begin{pmatrix} \omega + \mu + i\gamma & \sqrt{2}\kappa \\ \sqrt{2}\kappa & \omega + \mu - i\gamma \end{pmatrix}, \quad (10)$$

which represents a \mathcal{PT} -symmetric dimer [25–27]. From this, we conclude that the dynamics generated from a symmetric excitation in the latent sites $|1\rangle$ and $|2\rangle$ can only connect the site $|3\rangle$ with the bright mode $|B\rangle$. The discriminant now reads $\Delta = [(\Omega + \mu - \Omega_3)^2 + 8\kappa^2]^{1/2} = (-4\gamma^2 + 8\kappa^2)^{1/2}$ which shows that the evolution is stable if γ is selected in the range $\gamma \in (-\sqrt{2}\kappa, \sqrt{2}\kappa)$. The critical point $\gamma_c = \sqrt{2}\kappa$ corresponds to an exceptional point of second order of the full trimer associated with the bright invariant subspace. Thus, in the special case where $\gamma \in (-\sqrt{2}\kappa, \sqrt{2}\kappa)$, we have the real eigenvalues $\lambda'_{\pm} = \omega + \mu \pm (2\kappa^2 - \gamma^2)^{1/2}$. The imaginary parts of λ_j are displayed in Fig. 2.

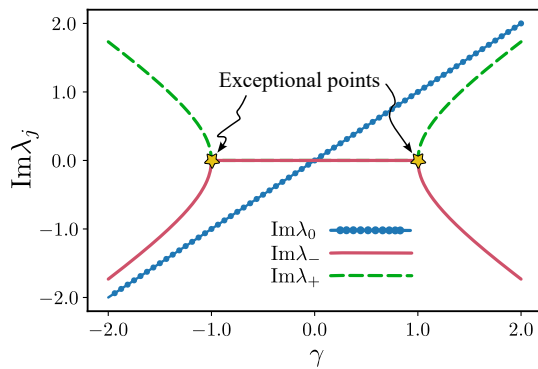


Fig. 2. Imaginary parts of the eigenvalues λ_0 , λ_+ and λ_- as a function of γ . The exceptional points are located at $\gamma_c = \pm 1$ for the set of parameters $\omega = 0$, $\mu = 1$ and $\kappa = 1/\sqrt{2}$.

In the case of symmetric initial excitation in the latent sites, $|\psi(0)\rangle = |B\rangle$, and in the absence of exceptional points, the evolved state is given by

$$|\psi(t)\rangle = e^{-iat} \left[\frac{\alpha(t)}{\sqrt{2}} (e^\chi |1\rangle + e^{-\chi} |2\rangle) + \beta(t) |3\rangle \right], \quad (11)$$

where $\alpha(t) = \cos(\eta t) - (i\delta/\eta) \sin(\eta t)$, $\beta(t) = -i\sqrt{2}\kappa \sin(\eta t)/\eta$, $\eta = \Delta/2$, $\delta = (\Omega + \mu - \Omega_3)/2$ and $a = (\Omega + \mu + \Omega_3)/2$. The local occupations are now

$$P_1 = \frac{e^{2\chi} |\alpha(t)|^2}{2}, \quad (12)$$

$$P_2 = \frac{e^{-2\chi} |\alpha(t)|^2}{2}, \quad (13)$$

$$P_3 = |\beta(t)|^2. \quad (14)$$

We thus observe a coherent and bounded energy exchange between the latent sites $|1\rangle$ and $|2\rangle$ and the singlet mode $|3\rangle$ even though the spectrum of the trimer has a complex eigenvalue λ_0 .

The cospectral analysis has revealed an exceptional point living in the bright sector of the trimer when the condition $\gamma = \gamma_c = \sqrt{2}\kappa$ is satisfied. In this case, the matrix given by Eq. (10) can be written as $H(\chi)_B = (\omega + \mu)I + N$, where I is the 2×2 identity matrix and

$$N = \gamma_c \begin{pmatrix} i & 1 \\ 1 & -i \end{pmatrix} \quad (15)$$

is nilpotent to second-order: $N^2 = 0$. The eigenvalues λ_{\pm} given by Eq. (8) become equal to $\lambda_c = \omega + \mu$ at $\gamma = \gamma_c$ and the (right) eigenvectors coalesce to $|\phi_c\rangle = |B\rangle - i|3\rangle$. If the initial state is given by the bright state $|\psi(0)\rangle = |B\rangle$, then $|\psi(t)\rangle = e^{-i(\omega+\mu)t} e^{-iNt} |B\rangle = e^{-i(\omega+\mu)t} (|B\rangle - itN|B\rangle) = e^{-i(\omega+\mu)t} [(1 + \gamma_c t)|B\rangle - i\gamma_c t|3\rangle]$. At the exceptional point, the local occupations grow polynomially as $P_1 = e^{2\chi}(1 + \gamma_c t)^2/2$, $P_2 = e^{-2\chi}(1 + \gamma_c t)^2/2$ and $P_3 = \gamma_c^2 t^2$.

Since the bright sector holds the stable dynamics, we now give numerical examples by solving $|\psi(t)\rangle = e^{-iH(\chi)t} |\psi(0)\rangle$, where $H(\chi)$ is given by Eq. (6) and $|\psi(0)\rangle = |B\rangle$ is the initial bright state of the trimer. Figure 3 plots the local occupations $P_j(t)$ for (a) $\chi = 0$ and (b) $\chi = 1/5$. In the first case, there is a periodic energy exchange between $(|1\rangle, |2\rangle) \leftrightarrow |3\rangle$. The energy is equally distributed between the two cospectral sites $|1\rangle$ and $|2\rangle$ during evolution. By changing the deformation parameter χ , this energy balance can be lifted, as shown in part (b) of the same figure. Thus, one can control the amount of energy each site receives by tuning χ appropriately. This fact is evident from the form of Eq. (12), Eq. (13) and Eq. (14), which shows that increasing χ has the effect of redistributing more energy into $|1\rangle$ while at the same time decreasing the energy content in site $|2\rangle$. Notice that P_3 is stable and independent of χ , as shown by the dashed-dot green lines in the figure. For suitable values of χ one can in fact generate an effective dynamics between $|1\rangle$ and $|3\rangle$ in which they exchange the same amount of energy much larger than the maximum value of P_3 .

4. CONCLUSIONS

In conclusion, we have introduced a minimal non-Hermitian trimer in which a cospectral pair of sites gives rise to latent symmetry and an exact decomposition into dark and bright sectors.

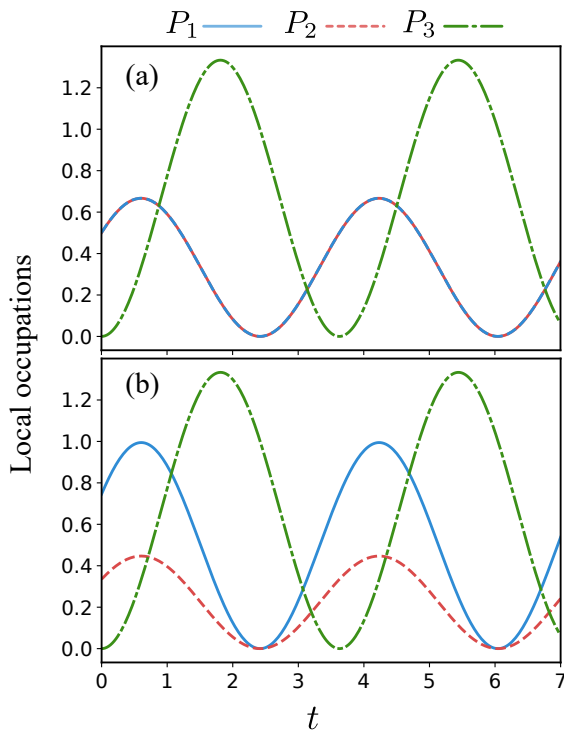


Fig. 3. Dynamics in the bright sector ($|\psi(0)\rangle = |B\rangle$) below the \mathcal{PT} phase transition point. Local occupations $P_j = |\langle j|\psi(t)\rangle|^2$ for (a) $\chi = 0$ and (b) $\chi = 1/5$. Other parameters are the same as in Fig. 2 and $\gamma = 1/2$.

The dark sector is formed by a spectrally isolated mode that remains decoupled from the singlet site, whereas the bright sector reduces exactly to an effective non-Hermitian dimer. For a suitable choice of onsite parameters, this reduced subsystem becomes \mathcal{PT} -symmetric and displays a regime of partial spectral reality, with two real eigenvalues coexisting with a complex dark eigenvalue. At the critical point, the bright sector hosts a second-order exceptional point embedded in the full trimer, leading to the characteristic polynomial-in-time dynamics associated with a Jordan block. Our numerical examples further show that, below the \mathcal{PT} -transition threshold, the deformation parameter χ provides a simple way to redistribute the local occupations while preserving bounded oscillatory exchange in the bright sector. These results establish the trimer studied here as a minimal analytically solvable platform in which latent symmetry, non-Hermitian mode selection, and exceptional-point physics coexist, and they suggest a useful route for mode engineering in photonic structures with asymmetric couplings.

5. FUNDING

This work was supported by the Brazilian agency CNPq (Conselho Nacional de Desenvolvimento Científico e Tecnológico).

REFERENCES

1. C. M. Bender and S. Boettcher, *Phys. Rev. Lett.* **80**, 5243 (1998).
2. R. El-Ganainy, K. Makris, M. Khajavikhan, *et al.*, *Nat. Phys.* **14**, 11 (2018).
3. A. Guo, G. J. Salamo, D. Duchesne, *et al.*, *Phys. Rev. Lett.* **103**, 093902 (2009).
4. C. E. Rüter, K. G. Makris, R. El-Ganainy, *et al.*, *Nat. Phys.* **6**, 192 (2010).
5. Ş. K. Özdemir, S. Rotter, F. Nori, and L. Yang, *Nat. materials* **18**, 783 (2019).
6. M.-A. Miri and A. Alù, *Science* **363**, eaar7709 (2019).
7. W. D. Heiss, *J. Phys. A: Math. Theor.* **45**, 444016 (2012).
8. A. J. Schwenk, “Almost all trees are cospectral,” in *New Directions in the Theory of Graphs*, F. Harary, ed. (Academic Press, New York, 1973), pp. 275–307.
9. M. C. Kempton, J. Sinkovic, D. Smith, and B. Z. Webb, *Linear Algebra. its Appl.* **594**, 226 (2020).
10. D. Smith and B. Webb, *Phys. A: Stat. Mech. its Appl.* **514**, 855 (2019).
11. J. Himmel, M. Ehrhardt, M. Heinrich, *et al.*, *ACS Photonics* **12**, 6570 (2025).
12. J. Himmel, M. Ehrhardt, M. Heinrich, *et al.*, *eLight* **6**, 3 (2026).
13. P. Lodahl, S. Mahmoodian, S. Stobbe, *et al.*, *Nature* **541**, 473 (2017).
14. R. Mitsch, C. Sayrin, B. Albrecht, *et al.*, *Nat. Commun.* **5**, 5713 (2014).
15. I. Söllner, S. Mahmoodian, S. L. Hansen, *et al.*, *Nat. Nanotechnol.* **10**, 775 (2015).
16. R. J. Coles, D. M. Price, J. E. Dixon, *et al.*, *Nat. Commun.* **7**, 11183 (2016).
17. B. Kannan, A. Almanakly, Y. Sung, *et al.*, *Nat. Phys.* **19**, 394 (2023).
18. C. Joshi, F. Yang, and M. Mirhosseini, *Phys. Rev. X* **13**, 021039 (2023).
19. C. Liedl, F. Tebbenjohanns, C. Bach, *et al.*, *Phys. Rev. X* **14**, 011020 (2024).
20. K. Li and P. G. Kevrekidis, *Phys. Rev. E* **83**, 066608 (2011).
21. K. Li, P. G. Kevrekidis, D. J. Frantzeskakis, *et al.*, *J. Phys. A: Math. Theor.* **46**, 375304 (2013).
22. S. V. Suchkov, F. Fotsa-Ngaffo, A. Kenfack-Jiotsa, *et al.*, *New J. Phys.* **18**, 065005 (2016).
23. R. Sharaf, M. Dehghani, and H. Ramezani, *Phys. Rev. A* **97**, 013854 (2018).
24. C. A. Downing, D. Zueco, and L. Martín-Moreno, *ACS Photonics* **7**, 3401 (2020).
25. J. D. Huerta Morales, J. Guerrero, S. López-Aguayo, and B. M. Rodríguez-Lara, *Symmetry* **8**, 83 (2016).
26. L. Jin, *Phys. Rev. A* **97**, 012121 (2018).
27. J. Naikoo, S. Kumari, S. Banerjee, and A. Pan, *J. Phys. A: Math. Theor.* **54**, 275303 (2021).

FULL REFERENCES

1. C. M. Bender and S. Boettcher, "Real spectra in non-hermitian hamiltonians having \mathcal{PT} symmetry," *Phys. Rev. Lett.* **80**, 5243–5246 (1998).
2. R. El-Ganainy, K. Makris, M. Khajavikhan, *et al.*, "Non-hermitian physics and PT symmetry," *Nat. Phys.* **14**, 11–19 (2018).
3. A. Guo, G. J. Salamo, D. Duchesne, *et al.*, "PT-symmetry breaking in complex optical potentials," *Phys. Rev. Lett.* **103**, 093902 (2009).
4. C. E. Rüter, K. G. Makris, R. El-Ganainy, *et al.*, "Observation of parity–time symmetry in optics," *Nat. Phys.* **6**, 192–195 (2010).
5. Ş. K. Özdemir, S. Rotter, F. Nori, and L. Yang, "Parity–time symmetry and exceptional points in photonics," *Nat. materials* **18**, 783–798 (2019).
6. M.-A. Miri and A. Alù, "Exceptional points in optics and photonics," *Science* **363**, eaar7709 (2019).
7. W. D. Heiss, "The physics of exceptional points," *J. Phys. A: Math. Theor.* **45**, 444016 (2012).
8. A. J. Schwenk, "Almost all trees are cospectral," in *New Directions in the Theory of Graphs*, F. Harary, ed. (Academic Press, New York, 1973), pp. 275–307.
9. M. C. Kempton, J. Sinkovic, D. Smith, and B. Z. Webb, "Characterizing cospectral vertices via isospectral reduction," *Linear Algebr. its Appl.* **594**, 226–248 (2020).
10. D. Smith and B. Webb, "Hidden symmetries in real and theoretical networks," *Phys. A: Stat. Mech. its Appl.* **514**, 855–867 (2019).
11. J. Himmel, M. Ehrhardt, M. Heinrich, *et al.*, "Eigenmodes of latent-symmetric quantum photonic networks," *ACS Photonics* **12**, 6570–6577 (2025).
12. J. Himmel, M. Ehrhardt, M. Heinrich, *et al.*, "State transfer in latent-symmetric networks," *eLight* **6**, 3 (2026).
13. P. Lodahl, S. Mahmoodian, S. Stobbe, *et al.*, "Chiral quantum optics," *Nature* **541**, 473–480 (2017).
14. R. Mitsch, C. Sayrin, B. Albrecht, *et al.*, "Quantum state-controlled directional spontaneous emission of photons into a nanophotonic waveguide," *Nat. Commun.* **5**, 5713 (2014).
15. I. Söllner, S. Mahmoodian, S. L. Hansen, *et al.*, "Deterministic photon–emitter coupling in chiral photonic circuits," *Nat. Nanotechnol.* **10**, 775–778 (2015).
16. R. J. Coles, D. M. Price, J. E. Dixon, *et al.*, "Chirality of nanophotonic waveguide with embedded quantum emitter for unidirectional spin transfer," *Nat. Commun.* **7**, 11183 (2016).
17. B. Kannan, A. Almanakly, Y. Sung, *et al.*, "On-demand directional microwave photon emission using waveguide quantum electrodynamics," *Nat. Phys.* **19**, 394–400 (2023).
18. C. Joshi, F. Yang, and M. Mirhosseini, "Resonance fluorescence of a chiral artificial atom," *Phys. Rev. X* **13**, 021039 (2023).
19. C. Liedl, F. Tebbenjohanns, C. Bach, *et al.*, "Observation of superradiant bursts in a cascaded quantum system," *Phys. Rev. X* **14**, 011020 (2024).
20. K. Li and P. G. Kevrekidis, "PT-symmetric oligomers: Analytical solutions, linear stability, and nonlinear dynamics," *Phys. Rev. E* **83**, 066608 (2011).
21. K. Li, P. G. Kevrekidis, D. J. Frantzeskakis, *et al.*, "Revisiting the PT-symmetric trimer: bifurcations, ghost states and associated dynamics," *J. Phys. A: Math. Theor.* **46**, 375304 (2013).
22. S. V. Suchkov, F. Fotsa-Ngaffo, A. Kenfack-Jiotsa, *et al.*, "Non-hermitian trimers: PT-symmetry versus pseudo-hermiticity," *New J. Phys.* **18**, 065005 (2016).
23. R. Sharaf, M. Dehghani, and H. Ramezani, "Effect of non-hermiticity on adiabatic elimination in coupled waveguides," *Phys. Rev. A* **97**, 013854 (2018).
24. C. A. Downing, D. Zueco, and L. Martín-Moreno, "Chiral current circulation and PT symmetry in a trimer of oscillators," *ACS Photonics* **7**, 3401–3414 (2020).
25. J. D. Huerta Morales, J. Guerrero, S. López-Aguayo, and B. M. Rodríguez-Lara, "Revisiting the optical \mathcal{PT} -symmetric dimer," *Symmetry* **8**, 83 (2016).
26. L. Jin, "Parity-time-symmetric coupled asymmetric dimers," *Phys. Rev. A* **97**, 012121 (2018).
27. J. Naikoo, S. Kumari, S. Banerjee, and A. Pan, "Pt symmetric evolution, coherence and violation of leggett–garg inequalities," *J. Phys. A: Math. Theor.* **54**, 275303 (2021).